Heliyon 6 (2020) e04574

Contents lists available at ScienceDirect

Heliyon

journal homepage: www.cell.com/heliyon

Research article

Characterization of composite material from the copolymerized polyphenolic matrix with treated cassava peels starch

Stephen Warui Kariuki [a,*], Jackson Wachira Muthengia [a], Millien Kawira Erastus [a], Genson Murithi Leonard [a], Joseph Mwiti Marangu [b]

[a] Department of Physical Sciences, University of Embu, P.O. Box 6-60100, Embu, Kenya
[b] Department of Physical Sciences, Meru University of Science and Technology, Meru, Kenya

ARTICLE INFO

Keywords:
Materials
Science
Lignocellulose
Oxidation
Esterification
Etherification
Rice husks
Maize stalk
Sugarcane bagasse

ABSTRACT

Conventional binders in the particleboards formulation involve use of formaldehyde resins. Epidemiologic studies show that formaldehyde is carcinogenic. Efforts to reduce formaldehyde emissions by use of scavengers has not been proven to reduce the emission. Molecular bonding of biobased adhesive molecules with lignocellulose materials provides an alternative way of producing composite material. In this study, maize stalk (MS), rice husks (RH) and sugarcane bagasse (SB) were used as sources of lignocellulose materials for particleboard formulation. SB, MS and RH were collected from their respective sites, sorted and dried. MS and RH were ground. Lignin content determination was done by drying lignocellulose material at 105 °C. Lignocellulose materials were prepared by hydrolysis of dried lignocellulose material with sodium hydroxide. Oxidized starch was prepared by oxidation of cassava peel starch using alkaline hydrogen peroxide. Particleboards were formulated through starch-lignocellulose polymerization at 60 °C compressed with 6.5 Nmm^{-2} pressure. Characterization of raw materials and formulated particleboards was done using XRD for mineralogical analysis, FTIR and NMR for elucidation of functional groups transformation. The results showed that esterification is the main process of chemical bonding in the particleboard formulation due to reaction between –COOH from starch and and OH- from lignocellulose. Etherification between hydroxyl groups from starch with hydroxyl groups from lignocellulose material. RH combined more through silication process with cassava peels starch than RH and SB showing materials containing high cellulose and hemicellulose content are more compatible. Composite materials formulated were used to produce medium density particleboards that can be used for making furniture and room partitioning.

1. Introduction

Solid wood, as a raw material to produce furniture, has become increasingly rare due to defforestation that causes desertification [1]. Lignocellulose sources such as crop residues have a large content of lignin, hemicellulose and cellulose [2]. Hemicellulose link lignin and cellulose in the lignocellulose matrix. The links are through hydroxyl and carboxylate groups. Hydroxyl and carboxylate groups are utilized during the condensation reaction [2]. Biobased polymers have been considered in the minimization of formaldehyde emission during making particleboards for furniture [3].

Copolymerizing natural polymers especially from crop residues emerges as an alternative in reduction of high cost of biodegradable polymeric materials [4] such as polyhydroxyalkanoate, polycaprolactone and polylactic acid. The high cost of these polymers is attributed to the huge cost involved during their extraction, fermentation and condensation [5]. Polysaccharides such as starch are obtained directly from cereals and tubers. They thus have a lower cost of production thus leads to an overall reduction in their cost of production. Starch, therefore, becomes affordable biobased polymers. The development of fully biodegradable polymers at low cost for the production of particleboards is currently a major challenge [5].

Chemical modification of starch is mainly done through oxidation, cationation and esterification. Oxidation using that increases carboxyl content [6], cationization of starch involves the introduction of the amino group in starch molecules [7, 8] and esterification involves substitution of hydroxyl groups with alkanoyl groups [9]. These methods decrease the starch crystallinity by breaking hydrogen bonding groups. Chemical modification of starch introduces new functional group in starch [10]. The functional groups include carboxyl, acetyl,

* Corresponding author.
E-mail address: stephowarui@yahoo.com (S.W. Kariuki).

https://doi.org/10.1016/j.heliyon.2020.e04574
Received 18 April 2020; Received in revised form 18 June 2020; Accepted 24 July 2020

hydroxypropyl, amine and amide which give specific properties. The chemical modification involves the formation of ester or ether, oxidation converts hydroxyl groups to carboxylic groups or carbonyl in addition to breaking of glycosidic links. Chemical modifications also involves but not limited to crosslinking and phosphorylation [11, 12], acetylation [13], carboxymethylation [14]. Physical modification of starch which includes heat-moisture treatment [15] disrupts the hydrogen bonding present in lignocellulose material.

Starch-based adhesives have limited applications in particleboard formulation attributrd to large number of free hydroxyl (-OH) that make them highly hydrophilic. Starch solubility can be reduced by chemical modification by reaction with alkali [16] as shown in Figure 1.

Starch is further plasticized with borax as a cross-linker. First, borax hydrolyzes in water form boric acid-borate ion. Secondly, it cross-links the hydrolyzed starch. The first step of borax hydrolysis [17] is as shown in Eqs. (1), (2), and (3).

$$H_2O_{(l)} + B_4O_7^{2-}{}_{(aq)} \leftrightharpoons OH^-{}_{(aq)} + HB_4O_{7(aq)}^- \quad (1)$$

$$B_4O_7^{2-}(aq) + 2H^+(aq) + H_2O(aq) \leftrightharpoons 4B(OH)_{3(aq)} \quad (2)$$

$$H_2O_{(l)} + B(OH)_{3(aq)} \leftrightharpoons H^+{}_{(aq)} + B(OH)_{4(aq)}^- \quad (3)$$

Borax form a cross-link between starch and lignocellulose polyols [18] as shown in Figure 2.

Lignin soaked in sodium hydroxide increases the tendency to copolymerize with other polymers such as starch [19]. Lignin has found application in the formulation of a green composite as a hardener in amine-cured epoxy materials [20]. Lignin is used to form plasticized starch which improves physical properties as well as mechanical characteristics of composite a material [21]. Composites consisting of copolymerized lignin and starch can be molded to produce particleboards [22]. Lignocellulose treatment with sodium hydroxide enhances the distribution of microfibers thus increasing the binding efficiency with the starch matrix [23].

Lignocellulose materials such as RH contain silica in amorphous form. Silica is hydrolyzed by alkali solutions such as sodium hydroxide (NaOH) forming sodium silicate ($Na_2O.SiO_2$) [24] as shown in Eq. (4).

$$NaOH_{(aq)} + SiO_{2(l)} \rightarrow Na_2O.SiO_{2(aq)} + H_2O_{(l)} \quad (4)$$

Sodium silicate hydrolyzes to silicic acid in the presence of water [25] as shown in Eq. (5).

$$Na_2O.SiO_{2(aq)} + 3H_2O_{(l)} \rightarrow 2NaOH_{(aq)} + H_4SiO_{4(aq)} \quad (5)$$

Silicic acid, like formaldehyde-based resins, undergoes polymerization to form an adhesive [18, 26] as shown in Eqs. (6) and (7)

$$(OH)_3Si{-}OH_{(aq)} + OH^-{}_{(aq)} \rightarrow (OH)_3Si{-}O^-{}_{(aq)} + H_2O_{(l)} \quad (6)$$

$$(OH)_3Si{-}OH(aq) + (OH)_3Si{-}O^-(aq) \rightarrow OH^-(aq) + (OH)_3SiO{-}Si(OH)_3(aq) \quad (7)$$

Starch was oxidized using hydrogen peroxide (H_2O_2) to form carboxyl and aldehyde functional groups. Silicic acid grafts with oxidized starch [27] as shown in Figure 3.

Copolymerization of polyphenolic matrix produces composite material that can be molded to particleboard. Major copolymerization sites on the modified naturally occurring polymers that include starch and components of lignocellulose like lignin hemicellulose and cellulose [28, 29] are shown in Figure 4.

This paper presents the characterization of particleboard made using RH, MS and SB using chemically modified starch from cassava peels. The particleboards, as reported by Kariuki, *et al.*, (2019) had the properties shown in Table 1 [28]. Particleboards formulated with rice husks bound with dextrinized starch (DS), hydrolyzed starch (HS), urea-oxidized starch (UOS) and oxidized starch (OS) were labeled as PBRDS, PBRHS, PBRUOS and PBROS respectively. Particleboard formulated with SB bound with dextrinized starch (DS), hydrolyzed starch (HS), urea-oxidized starch (UOS) and oxidized starch (OS) were labeled as PBSDS, PBSHS, PBSUOS and PBSOS respectively. Particleboard formulated from MSs bound with dextrinized starch (DS), hydrolyzed starch (HS), urea-oxidized starch (UOS) and oxidized starch (OS) were labeled as PBMDS, PBMHS, PBMUOS and PBMOS respectively.

2. Materials and methods

2.1. Materials

Lignin sources were collected from three geographical areas for cereal straws; Maize stalks were obtained from Arahuka Farm in Nakuru County, Kenya (0° 18′ S, 36° 4′ E), Sugarcane residues were collected from Muhoroni Sugar Company in Kisumu County, Kenya (0° 5′ S, 34° 46′E) while RH were collected in Mwea Rice Millers (0° 37′S, 37° 20′ E), Kirinyaga county. MS was chopped and milled to <10 mm in particle size. SB was used in same form collected from the disposal site. RH were reduced to less than 10 mm in particle. Crop residues dried at 105 °C in an oven untill no change in mass was recorded. Cassava tubers were obtained from Thika, Kiambu County. Peels from cassava tubers were harvested and rinsed with distilled water.

2.2. Lignin determination

Lignin in lignocellulose material was determined in accordance with Klason method [30]. 10.00 g of the ground lignocellulose material was weighed and labeled L_1. 14 ml of 13.4M sulphuric acid at 25 °Cwas then added to L1 while stirring for 30 min. The resultant mixture was then allowed cool for 2 h, washed with 450 mL of deionized water in a cornical flask. The resultant mixture was then boiled for 4 h under reflux, filtered and residue rinsed using deionized water. The residue was oven dried at 105° C to a constant mass. The dried residue was cooled, weighed and the mass recorded as lignin content [31]. The dried insoluble substance was labeled L_2. The percentage of lignin content was calculated using Eq. (8).

$$\text{Percentage lignin content} = \frac{L_2}{L_1} \times w \times 100 \quad (8)$$

where w is the mass of lignocellulose used.

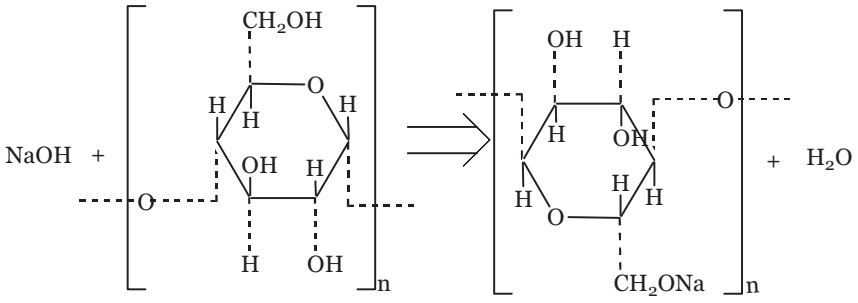

Figure 1. Alkalization of starch with sodium hydroxide.

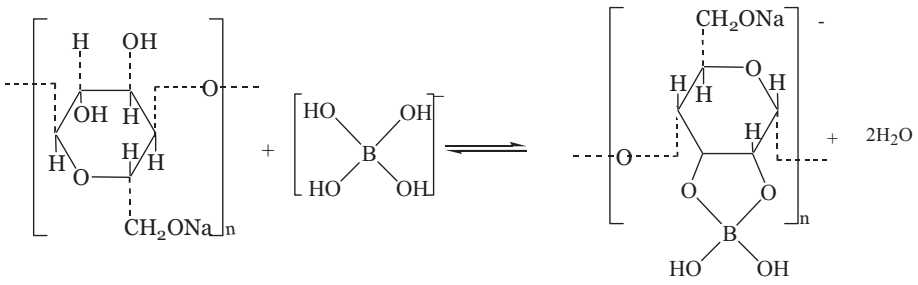

Figure 2. Crosslinking starch using borax.

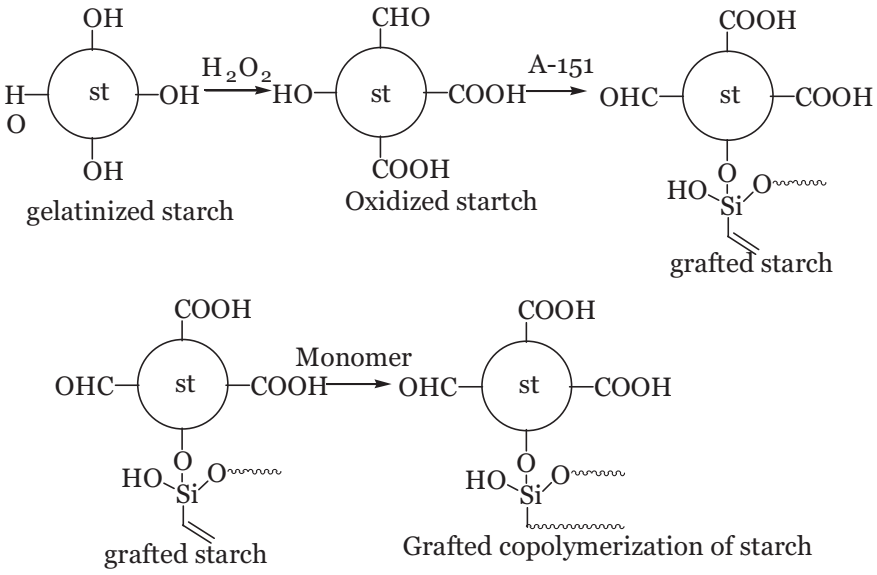

Figure 3. Reaction pathway for the synthesis of starch-based adhesive.

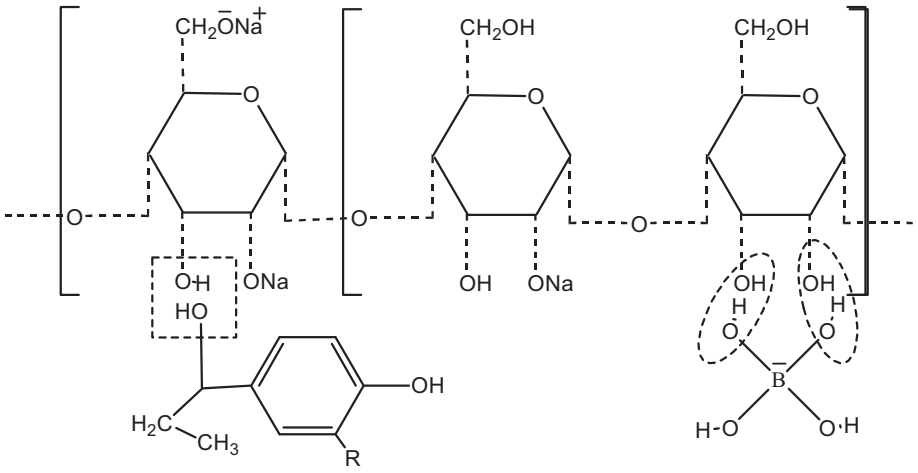

Figure 4. Interaction mechanism between hydrolyzed starch and oxidized lignocellulose materials.

2.3. Preparation of oxidized starch

12.50 g of ground starch and 5.00 g Na_2CO_3 was mixed and 40.0 mL 20 % H_2O_2 in a 200 mL beaker while stirring for 30 min. The resulting mixture was dried to a constant mass at 60 °C. The resultant solid was pulverized to a fineness of 100 microns. The process was done in triplicates [32]. The three portions were prepared as P1, P2, and P3.

2.4. Preparation of lignocellulose material

The preparation of lignocellulose material for the study was done following Sluiter *et al.,* 2016) [33]. 70 g of dried lignocellulose material was soaked in 1400 mL of 20% hydrogen peroxide in a 2000 mL beaker at pH 11.5 maintained using sodium hydroxide. The mixtures were stirred using a magnetic stirrer maintained at 25 °C for 15 min then filtered with

Table 1. Average values of density, moisture content (MC), water absorption (WA), thickness swelling (TS), internal bond (IB), modulus of rupture (MOR) and modulus of elasticity (MOE).

Boards	Density in (g/cm^3)	MC in (%)	WA in (%)	TS in (%)	IB in (Nmm^{-2})	MOR (Nmm^{-2})	MOE (Nmm^{-2})
PBRDS	0.623^{a}	9.700^{b}	74.67^{a}	20.63^{b}	1.623^{a}	13.553^{a}	2875.67^{b}
PBRHS	0.612^{a}	9.587^{a}	76.33^{a}	19.32^{a}	1.613^{a}	13.630^{a}	2651.61^{a}
PBRUOS	0.621^{a}	9.487^{d}	68.61^{c}	19.12^{d}	1.710^{c}	14.323^{c}	2891.67^{d}
PBROS	0.622^{a}	9.593^{c}	64.67^{b}	18.59^{c}	1.657^{b}	13.770^{b}	2806.67^{c}
PBSDS	0.627^{b}	9.770^{b}	69.27^{b}	19.88^{a}	1.677^{a}	13.630^{b}	2907.68^{b}
PBSHS	0.608^{a}	9.543^{a}	66.67^{a}	18.94^{a}	1.720^{a}	13.880^{a}	3175.71^{a}
PBSUOS	0.611^{ab}	9.553^{c}	71.04^{d}	18.46^{c}	1.950^{c}	14.320^{d}	3329.93^{d}
PBSOS	0.619^{ab}	9.567^{a}	61.33^{c}	18.23^{b}	1.820^{b}	14.134^{c}	3229.08^{c}
PBMDS	0.622^{b}	9.843^{b}	83.87^{a}	23.43^{b}	2.367^{b}	13.960^{b}	2364.20^{b}
PBMHS	0.604^{a}	9.577^{a}	81.33^{a}	22.77^{a}	2.220^{a}	14.380^{a}	2508.34^{a}
PBMUOS	0.615^{a}	9.593^{d}	78.68^{c}	19.44^{d}	2.370^{bd}	14.830^{d}	2716.57^{d}
PBMOS	0.621^{c}	9.763^{c}	72.67^{b}	19.31^{c}	2.343^{c}	14.720^{c}	2672.27^{c}

Values shown indicate the means and the superscript with same small letters indicate that they are not significantly different and different small letters indicate they are significant different with respect to their mean.

Buchner funnel. The solid part was rinsed using deionized water. The solid was oven dried at 105 °C to a constant weight.

2.5. Particleboard formulation

Particleboard was formulation in accordance to starch–lignin polymer preparation [34] with slight modification. 12.5 g of starch was added to a pre-heated 250 cm^3 of 0.4 M NaOH solution at 40 °C placed on a heater in a 500 cm^3 Pyrex beaker while stirring. The temperature of the resultant mixture was raised to 55 and 60 °C and remained at that range for further 15 min. To the resultant mixture 2.00 g of sodium borate (borax) was while stirring for further 15 min. The hot mixture was put into a 1000 cm^3 plastic beaker and 70 g of MS added and stirred with a wooden stick for 10 min. The resulting composte material was allowed to cure for 2 h at 25.0 °C and transferred to an iron mold lined with 1 mm polyethene sheet. The composite material was compressed for 6 min at 6.5 Nmm^{-2} pressure at 30 °C. The mold was air-dried for 48 h to to a constant mass. The air dried mold was further oven dried at 60.0 °C to a constant mass. Procedure replicated separately for RH and SB. The procedure was done in triplicate for each lignocellulose material. The resultant particleboards were labeled as PBROS, PBSOS and PBMOS for formulations with RH, SB and MS respectively.

3. Characterization and testing

3.1. Nuclear magnetic resonance (NMR) analysis

The solid-state ^{13}C CP-MAS NMR spectra for cassava peel starch-NaOH-borax adhesive were used with Bruker AV400 spectrometer operated at 100.61 MHz frequency using a 4 mm wide-line MAS probe. Samples were spunned at 10 kHz in zirconia rotors to obtain spectra utilizing a CP-MAS pulse sequence equiped with 1 ms contact time and a 5 s recycle delay. The spectra was obtained by averaging 1800–4000 scans. Chemical shift (δ) was refered to deuterochloroform ($CDCl_3$) as a control. Sample spectra were determined using literature reference spectra to identify main molecular groups.

3.2. X-ray diffraction (XRD) analysis

10.00 g of the ground sample of lignocellulose material and cassava peels starch was put in six sample cell holders. The sample holders were tapped carefully to ensure the particles were parked to avoid displacement which affects peak shifts. They were then loaded for analysis of minerals using data collector software. The result of the analysis of minerals present in each sample was obtained using a Bruker D_2 phaser diffractometer for analysis. Data was shown in single-phase collection of XRD patterns for most intense 3D values in form of interplanar spacings (D) tables, mineral name and relative intensities ($^{I}/_{Io}$) [35]. Sample spectra were related to literature reference spectra to identify the mineral.

3.3. Fourier transform infrared (FT–IR) spectroscopy

FT-IR spectroscopy was done using direct transmittance with attenuated total reflectance (ATR) accessory (IRT Laser-100 SHIMADZU). Spectrum were scanned at a resolution of 4 cm^{-1} between 600 cm^{-1} to 4000 cm^{-1}. The background spectrum for each sample was collected before sampling. Particleboards were conditioned to 102 °C for 24 h in an oven. All the infrared spectra were obtained with an FTIR spectrometer by use of the KBr disk method. Spectra recordind was done using 32 scans at an average at a resolution of 4 cm^{-1}. Untreated and treated samples were pulverized to 100 mesh. 200 mg of samples were oven dried at 60 °C for overnight. Ground samples were converted into a ball and placed in a desiccator with phosphorus pentoxide (P_2O_5). Samples heat-treated with similar mass losses were used for spectra collection. Each treatment-time-species combination gave 1 spectrum. The spectra were collected with 1.50 mg–1.55 mg material using attenuated total reflectance. The sample spectra were related to literature reference spectra to identify functional groups [36]. The samples of the particleboards were scanned using the ATR with less emphasis on the sample preparation. ART avoids any reactions that affect the structure of the functional groups during its preparation.

4. Results and discussion

4.1. Lignin content

Lignin in MS, SB, and RH was determined. SB contains the highest percentage of lignin that range from 21.5 ± 2.1 %, MS and RH had 11.4 ± 1.2 % and 15.9 ± 6.2 % respectively. Lignin content determines the WA and TS of particleboards. Lignin incorporated to composite material results into reduced WA and TS [37]. Lignin is a natural adhesives [38, 39]. Lignin has few free hydroxyl (-OH) groups that bond with water forming hydrogen bonding [40]. Hydroxyl groups from materials such as lignin are utilized during copolymerization. These findings indicate that the levels of cellulose and hemicellulose make up a higher percentage of the lignocellulose material. Cellulose and hemicellulose act as filler material in the manufacture of the composite material.

4.2. Fourier transform infrared(FT-IR) spectroscopy

Figure 5 show the main absorption bands in oxidized cassava peel starch, raw cassava peel starch, PBSOS, PBROS, PBMos, raw SB, raw RH and raw MS.

Major peak was observed at 3415.06 cm^{-1} associated to hydroxyl (-OH) groups and primary amine groups in the compounds. A peak at 1625.98 cm^{-1} was attributed to –OH bending mainly observed as a result of WA. Peaks attributed to –C-H from starch, cellulose, hemicellulose, and lignin were observed at 2484.4 cm^{-1} and 1362.7 cm^{-1}. A peak corresponding to –C=O vibration appeared at 1229.64 cm^{-1}. Another peak at 1102.4 cm^{-1} that relate to -C-O stretching was observed. The reduction of –OH peaks at 3414.06 cm^{-1} and corresponding rise of peak size at 2484.36 cm^{-1} for -C-O was observed. This change was attributed to utilization –OH as they are converted to ethers and esters. Hydroxyl (–OH) group spectra remained is due to the presence of sodium hydroxide (NaOH) utilized during pre-treatment. It also associated with water (H_2O) formed during the condensation reaction and hydrolysis of borax in sodium hydroxide formation to form boric acid. Peaks that appeared at 1150 and 950 cm^{-1} were associated to B–OH due to the hydrolysis of sodium borate. Staroszczyk and Janas (2010) reported a similar peak at around 1194 cm^{-1} associated with B–O–H, characteristic for the trigonal planar molecules of boric acid [41].

Reduction in peak size at 3414.06 cm^{-1} –OH is due to its reaction during condensation reaction. With an increase in peak size at C=O and C–O, it showed that there was the formation of an ester. The peak associated with -C-H increased due combination of -C-H from lignocellulose matrices and cassava peels starch. A decrease in the major peak at 995.05 cm^{-1}attributed to C–OH reveals the loss of –OH from glucose utilized in silication reaction. This change increased peak intensity at 1082.01 cm^{-1} associated with -C-O-C in glycosidic bond found in starch as a result of interaction between silicic acid and starch. Staroszczyk and Janas (2010) obtained similar results during the modification of potato starch with silicic acid [41]. The decrease in peak size at 1345.5 cm^{-1} is attributed to the crosslinking of starch with hydrolyzed borax, this led to occurence of a peak at 1259.74 cm^{-1} associated to C–O–B–O–C. This shows, therefore, B–O–H was transformed through a condensation reaction with –OH from lignocellulose material. Staroszczyk and Janas (2010) reported similar transformations of B–OH to C–O–B–O–C during boration of potato starch.

Peaks observed between 850 and 900 cm^{-1} are attributed to β-(1–4)-glucosidic linkages of cellulose [42]. Similar results were obtained in analysis of corn stalk with an absorption band at 895cm^{-1} [43]. The glucosidic linkage is hydrolyzed with alkaline catalyst to form carbohydrate chains from glycoconjugates. Chemical shift observed is due to extensive lignin and hemicellulose removal during pretreatment with sodium hydroxide (NaOH) that exposes cellulose. Hydrolysis glucosidic linkage alter the cellulose structure which causes hydrogen bonding rearrangement in the network [44].

Discussion above clearly shows there were bond formation as a result of esterification between carboxylic groups from cassava peels starch and hydroxyl groups from lignocellulose material, silication process, the reaction between hydroxyl groups from silicic acid with carboxylic groups from cassava peels starch, crosslinking of starch with hydrolyzed borax through condensation reaction between hydroxyl groups from borate and lignocellulose material. These are the major bond formation that resulted in particleboard formulation.

4.3. Mineralogical composition of starch, lignocellulose and composite material formed

Figure 6 shows results of XRD analysis for the cassava peel starch, MS, SB, RH, and laboratory starch determined in the study.

Figure 6 shows the diffractogram of untreated SB, RH, and MS. XRD patterns of untreated SB, RH, and MS had peaks (2θ) at 15.3°, 17.5°, and 23.1° which is a typical identity of cellulose. Crystallinity is attributed to amide bonds as well as hydrogen bonding between amino (-NH_2), and hydroxyl (-OH) groups from starch and cellulose. The intensity of the crystallinity depends on the amount of cellulose. The composite material used to formulate particleboards showed the highest peaks. An increase in peaks showed the coexistence of cellulose in both starch and lignocellulose material [45].

The decrease in starch crystallinity is attributed to lignin incorporated in starch. Lignin exists as an amorphous polymer. Cassava peels starch portrayed C-type crystallinity of A-type. The starch analysis showed 2θ = 17.5°. The peak is attributed to the presence of amylopectin

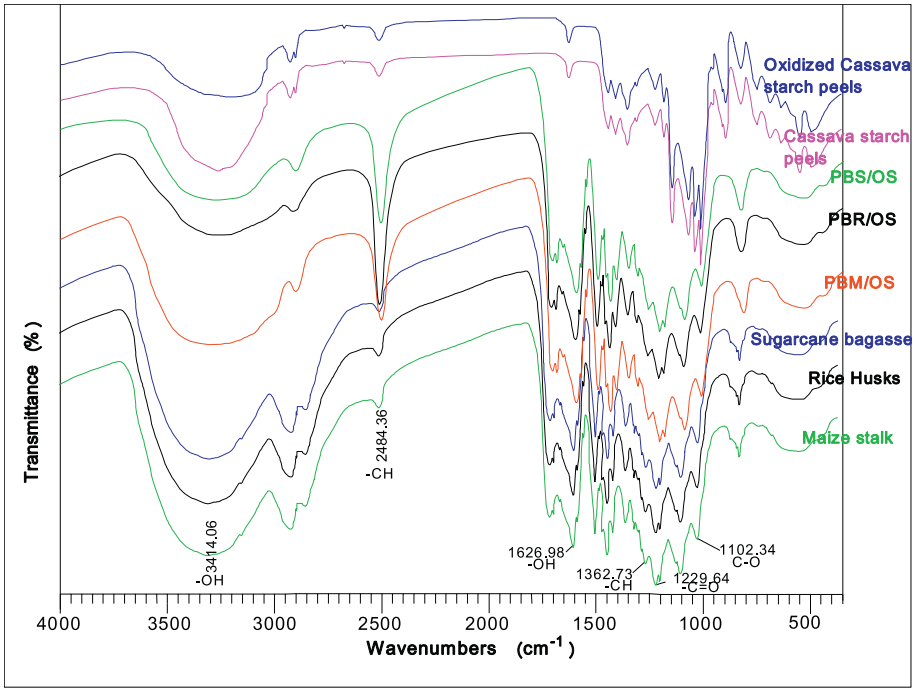

Figure 5. FTIR spectra for cassava starch, rice husks and the board made from rice husks and cassava starch.

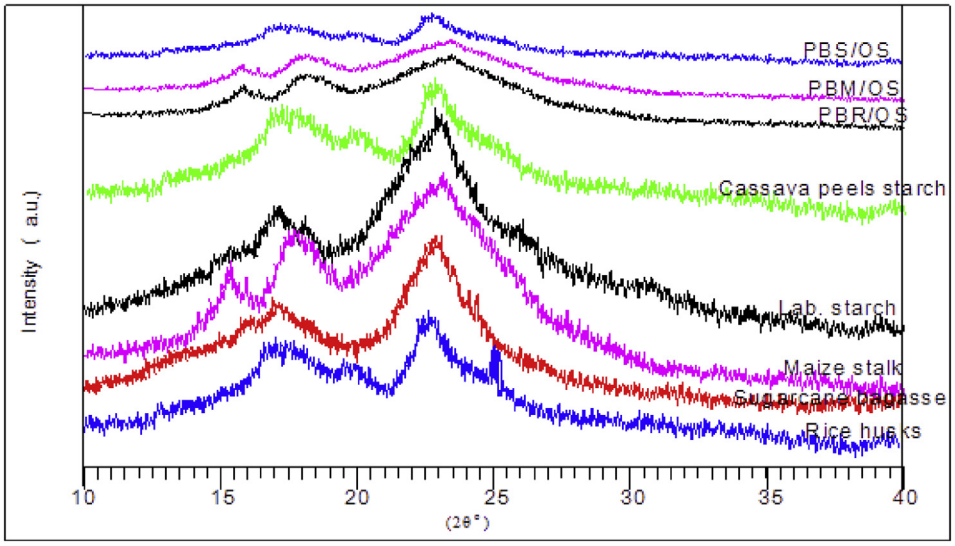

Figure 6. X-ray diffraction of rice husks, sugarcane bagasse, maize stalk, and lab starch.

recrystallization (B-type crystallization). Amylose diffraction spectra were observed at $2\theta = 23.1^{\circ}$ denoted as V_H-type. Addition of lignocellulose material reduced the V_H –type peak due to lignin present. Reduction in crystallinity of B-type index was observed in all samples that was dependent on the concentration of lignin. The partial decrease in peak size shows low compatibility of cassava peel starch with lignin. This is due to strong attraction between phenolic groups in the lignin. Morphology analysis of gelatinized starch showed homogeneity between sodium hydroxide and borax as used as a plasticizer. Lignocellulose material made the surface rough which is observed in all composite materials. The above observation is similar to the ones observed by Uthumporn, *et al.*, (2012) who were working on hydrolysis of cereal starch granules using sodium hydroxide [46].

XRD spectra for RH showed extra spectra at $2\theta = 22^{o}$ which is attributed to silica in the form of SiO_2 and 25.23^{o} attributed to sodium silicate. RH are known to have a high ash content than the other materials under study. Further, the ash is documented to have a high silica content [47]. Similar findings were found by Fernandes, *et al.*, (2017) while characterizing SiO_2 from rice husks ash (RHA) [48]. The same observation was made in characterization of amorphous SiO_2 production from RHA [49]. The presence of this SiO_2 confirmed the appearance of the results obtained from the FTIR spectra in Figure 5. Silica can be utilized in bonding by converting it to silicic acid. Silicic acid has been utilized as an adhesive and can be crosslinked with organic molecules through biomineralization [50].

The discussion above shows a reduction in crystallinity in cassava peels starch on addition of lignocellulose material. This is due to etherification of hydroxyl groups from starch and hydroxyl groups from phenolic groups in lignin in lignocellulose material. Reduction in crystallinity is attributed to esterification due to reaction between carboxylic groups from oxidized starch with hydroxyl groups in phenolic groups from lignin in lignocellulose material Copolymerization through etherification and esterification between cassava peels starch and lignocellulose material form a covalent bond. Covalent bonding is one of the major molecular bonds in the formulation of particleboards.

4.4. NMR analysis results for raw materials and formulated particleboard

NMR analysis for MS, SB, RH and formulated particleboards was done and the results shown in Figure 7.

NMR analysis for MS, SB, RH, and formulated particle boards are presented in Table 2.

Particleboards formulated from SB showed major spectra at 24.7 ppm associated with CH_3 in acetyl groups of hemicelluloses and lignin. This spectrum is associated with CH_3CO, hydroxylamines, oximes and hydroxamic acids. At 46 ppm peak was observed that is related to disilene. At 64 ppm a peak associated with CH_2- in RCH_2OH was also observed from C_6 carbon of crystalline cellulose. Signals at 60 ppm–105 ppm are attributed to the carbohydrates from starch, hemicellulose and cellulose. An increase in the peak size attributed to the combination of starch, cellulose, lignin and hemicellulose molecules [51]. Other peaks observed were at 72 ppm associated with C_5, C_3 and C_2 of hemicellulose and cellulose. Spectra between 60 to 80 ppm are attributed to the etherification of aromatic rings [52]. The peak at 82 ppm associated with alkynes, 116 ppm and 146 for C_1 and C_6 associated with aromatic and carbon of double bonds on the side chain. The peak at 131 ppm is associated with an alkene, 172 and 176 ppm were observed for carbonyl in ester and acid and carbonyl. NMR peaks around 170 ppm are a result of aliphatic esters and aliphatic carbonyls [53].

Particleboards formulated with RH and modified starch showed major peaks at 11.4684 which is associated with RCH_3. A peak observed at 25.3603 ppm is associated with C in R_2CH_2. A peak observed at 32.9433 ppm is attributed to C in CH_3CO- whereas at 42.2854 ppm associated with C in RCH_2NH_2. The peak at 57.4267 ppm is associated with C in methoxy group [54] and 64.6399 ppm associated with C in RCH_2OH of C6 carbon of crystalline cellulose, 72.2532 and 82.4446 ppm associated with C in alkynes and hemicelluloses [55]. A peak was observed at 88.5717 ppm is associated with the presence of C in RCH_2O-, 104.7991 and 119.3584 ppm associated with C in alkene, 128.8219, 137.0418, 145.2929, and 150.7820 ppm associated with aromatic [56]. Spectral lines observed at 167.7981, 170.2550, 171.8323, 172.8332, 177.2010 and 181.4474 ppm are associated with carbonyls in ester and carboxylic acid.

Particleboards formulated with MS gave major spectra peaks at 24.7234 ppm in R_2CH_2, 46.9262 ppm for C in RCH_2NH_2, 64.5793 ppm for C in RCH_2OH. The strong peak at 58–68 ppm is associated with C_6 [57], 72.3745 ppm from C_2 C_3, C_5 of cellulose. Peaks between 68 to 78 ppm attributed to the interaction of C_5, C_3 and C_2 during reaction between hydrolyzed starch and high amylose starch [58]. Carbon of lignin and 82.5390 ppm associated with C in alkynes, 104.5888 ppm associated with C_1 of single helix part in starch granules, 116.5982, 131.6730 and 146.0503 ppm are attributed to the presence of aromatic. 172.7332 and 176.5356 ppm are identified with carbonyls in ester and acid.

Spectrum acquired on SB, RH and MS showed the presence of peaks at 21.5 and 173.6 ppm an evidence that hemicellulose is present. The peaks

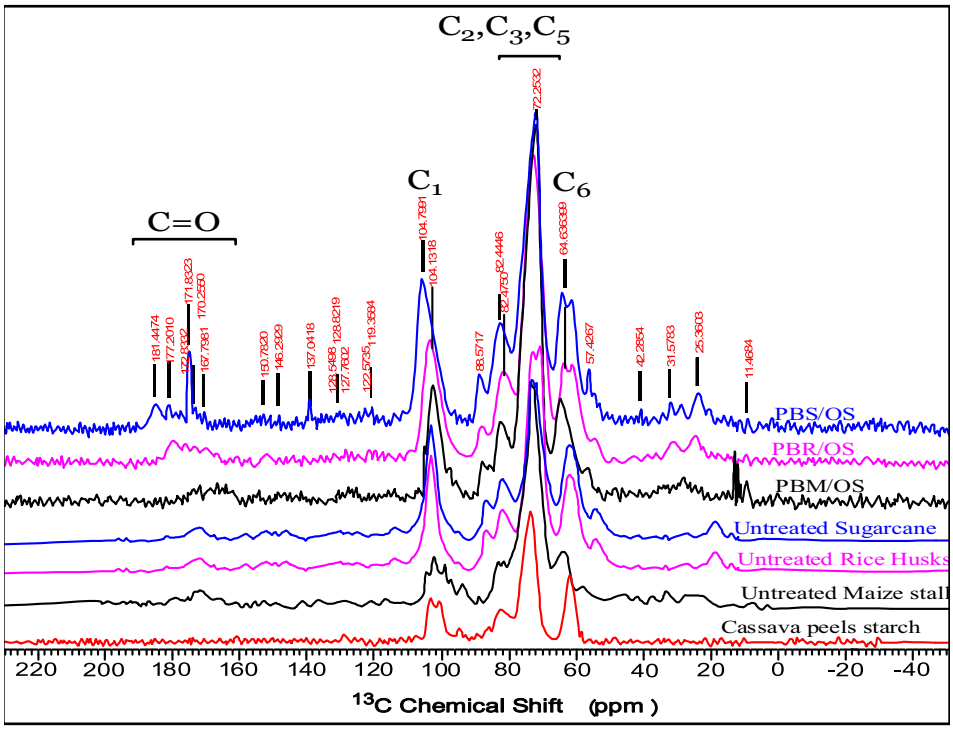

Figure 7. NMR spectra for cassava peel starch, maize stalk, rice husks, sugarcane bagasse and particleboards formulated.

at 50 ppm–120 ppm are associated with the presence of hemicellulose [59]. There were slight changes in spectra size attributed to lignin due to delignification during sodium hydroxide treatment. Cellulose extracted from sugarcane was identified with the following peaks: 64.8 ppm. 62.4 ppm, 72.5–74.8 ppm, 82.3–83.7 ppm, 88.8 ppm and 104.7 ppm [60]. Intensity of spectra increased between 70 ppm to 76 ppm which is attributed to combination of C_2, C_3 and C_5 from cassava peel starch and cellulose from lignocellulose material. Cassava peel starch and cellulose polymers undergo condensation reaction to form copolymers that increases C_2, C_3 and C_5 in the chain.

Peaks concentrated between 50 and 120 ppm attributed to the three main components of lignocellulose material. Peaks at 62.5 and 83.4 ppm are mainly attributed to cellulose carbons, while those at 64.7 and 87.8 ppm are mainly associated to cellulose carbons. Peaks observed between 100 ppm to 200 ppm are associated with lignin. Lignin specta are broader because of their complexity in chemical nature and existence of structure

Table 2. MAS 13C NMR chemical shifts and attributed functional groups.

^{13}C chemical shift (ppm)	Chemical group
11.47	RCH_3
24.7	CH_3, C in R_2CH_2
25.36	C in R_2CH_2
32.94	C in CH_3CO
42.29	C in RCH_2NH_2
46.93	C in R_2CH_2
46.92	CH_3CO, hydroxylamine, oximes, hydroxamic acid
57.43	C in RCH_2OH of C_6 carbon of crystalline cellulose
64.57	C in RCH_2OH
72.37	C_2, C_3, and C_5 of cellulose and hemicellulose and hemicellulose and $OC_\alpha H_2$ carbons of lignin
82	Alkynes and hemicelluloses
	$OC_\alpha H_2$ carbons of lignin
88.57	C in RCH_2O
104.7991 and 119.3584	C in alkene
116 and 146	C_1 and C_6 associated with aromatic and carbon of double bonds on the side chain
128.8219, 137.0418, 145.2929, and 150.7820	Alkene and aromatic in lignin and its derivative
131	Alkene
172 and 176	Carbonyl in ester and acid and carbonyl
128.8219, 137.0418, 145.2929,	C in alkene
150.7820	aromatic
167.7981, 170.2550, 171.8323, 172.8332, 177.2010 and 181.4474	carbonyls in ester and carboxylic acid

that is disordered. Signals at 21.4 ppm and 173.5 ppm are attributed to hemicellulose carbons and peak at 56.3 ppm is associated to methoxy (OCH_3) found in lignin [61]. In comparison, the result showed that cassava peels starch and lignocellulose material combined to form a composite material. Results showed that –OH, H–O–B and N–H were broken and formation of C–N, C–O–B and C=O were formed. C–N and C=O appear between 150 to 200 ppm.

The emergence of peaks related to carbonyl groups in esters and polypeptide bonds is attributed to the reaction between cassava peels starch and lignocellulose material. Carbonyl groups are produced through the esterification of carboxylic acid from starch and hydroxyl (-OH) from aromatic groups of lignin, cellulose and hemicellulose through condensation reaction. Polypeptide bond is formed from the reaction between amine groups from crude proteins in cassava peels starch and hydroxyl groups from lignocellulose material through condensation reaction. Condensation reaction results in copolymerization between natural polymers in lignocellulose material and cassava peel starch that was used in the formulation of the particleboards.

4.5. SEM analysis of starch and particleboards

SEM analysis of untreated cassava peel starch was determined and the results shown in Figure 8.

Cassava peels starch exists in mixed patterns of elliptical-shape, round crystalline form and amorphous parts. Different shapes are as a result of hydrogen bonding within amylopectin molecules. Hydrogen bonding also exists between amylose and amylopectin. Pores increase the surface area where the chemical reaction occurs. Porosity significantly influences starch chemical reactivity [62]. Microscopic pores make the surface of cassava peel starch appear smooth. Molecules in the starch granules and amorphous region contain hydroxyl groups that are required during the chemical reaction. Break down granules to increase starch surface area.

SEM analysis for the gelatinized starch was done and the image shown in Figure 9.

Figure 9 show dispersion of cassava peel starch granules treated with sodium hydroxide (NaOH) solution. Sodium hydroxide (NaOH) promotes swelling and dispersion of starch granules. Chemical treatment of starch using sodium hydroxide was utilized to form a gel which exposes the –OH groups used during copolymerization. NaOH reacts with hydroxyl (-OH) groups from starch to form sodium salts. The formation of sodium salts breaks up the hydrogen bonding between starch molecules leading to exposure of more hydroxyl groups [63, 64]. Change in morphology, therefore, is attributed change of some OH groups to $O^{-}Na^{+}$ and alkali hydrolysis of some glycoside bonds. NaOH reduces the rigidity and stability of cassava peels starch. The mobility of cassava peels starch results into loss of granular form [65]. Gelatinized starch was used as a binder in this study.

SEM micrographs of formulated particleboards with SB, MS and RH bound with oxidized starch are shown in Figure 10.

Figure 10 shows SEM images of surfaces of the particleboards formulated in this study. All particleboards showed an interaction between gelatinized starch and the lignocellulose materials. The variation in density in Table 1 is attributed to the reaction between starch and the lignocellulose material. SEM analysis for the particleboards showed larger voids between the SB fiber materials and cassava peels adhesive. Voids are formed due to insufficient interaction between lignocellulose material and the adhesive. SB had the highest lignin content among the three lignocellulose material. Lignin is hydrophobic with few hydroxyl groups that are used in bonding with starch molecules. Low cellulose content reduces the binding area of adhesive. Particleboards formulated with SB appeared rough due to protrusions roughness of the lignocellulose material used. Carboxylic groups in oxidized starch react with –OH of the lignocellulose material. Starch hydrolysis with sodium hydroxide only broke the hydrogen bonding. Gelatinized starch was trapped in the SB matrix resulting in a lower degree of penetration. Interaction between two polymers reduces the mobility of an adhesive [66].

SEM micrographs of particleboards formulated with MS showed smaller voids between lignocellulose material and adhesive. The presence of cellulose and hemicellulose fillers provided extra interaction sites between lignocellulose material and the adhesive. Cellulose content increases fiber tensile properties through oxidation [67]. Hydroxyl (-OH) groups from cellulose are transformed to aldehydes and carboxylic acid [28, 68]. Carboxylic (-COOH) groups react with hydroxyl (-OH) groups in cassava peel starch to form a covalent bond through esterification. Particleboards formulated from MS showed smooth surfaces due to cementation from hemicellulose and lignin. Similar findings were reported when RH was treatment with using sodium hydroxide (NaOH) [69].

SEM analysis of particleboards formulated with RH showed a more undulated surface associated with regularly spaced conical-like protrusion. This is also due to SiO_2 adhesion as a result of the reaction between silica and sodium hydroxide to form sodium silicate. Small pores are associated with the cementing of cellulose and hemicellulose. Sodium silicate acts as an adhesive and a filler for voids to make the surface have a smoother appearance.

Images in SEM analysis explain the different spectral lines in NMR analysis. The reaction between the cassava peel adhesive and lignocellulose material relates to the difference in appearances on the surface of the particleboard formulated. Spectra at 72.2532 ppm increased from those of raw materials to those of particleboards. The change is associated with the combination of cellulose and starch materials. The interaction between MS and cassava peel starch showed the highest peak. The reaction between lignocellulose material and modified starch determines the mechanical properties of the formulated particleboards. Higher compatibility results in a higher modulus of rupture (MOR). The reaction

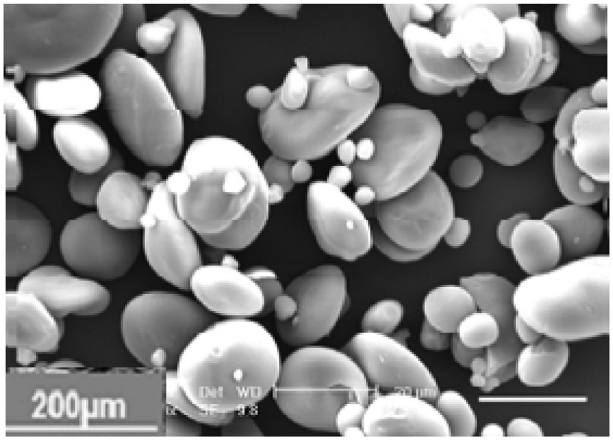

Figure 8. Sem analysis of raw starch from cassava peels.

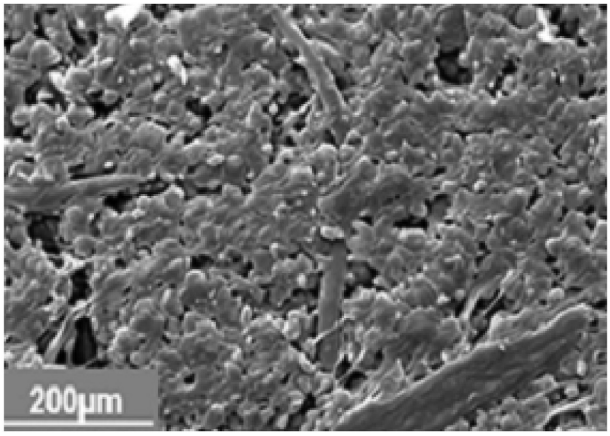

Figure 9. SEM analysis of gelatinized starch.

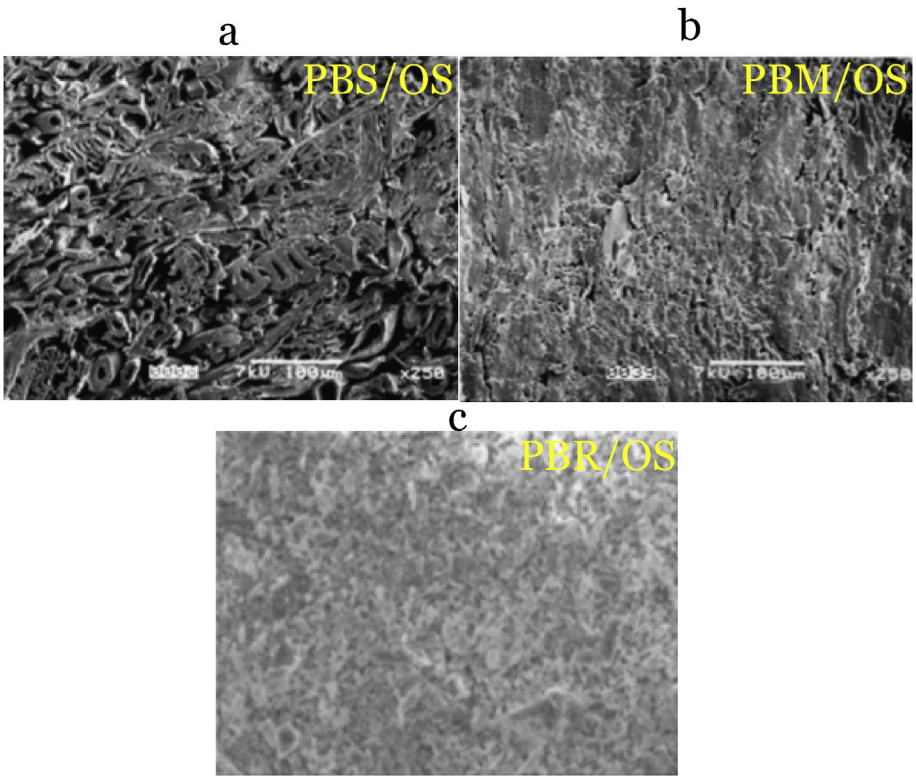

Figure 10. SEM analysis of a) PBS/OS, b) PBM/OS and c) PBR/OS.

between RH and cassava peels starch as clearly indicated in NMR spectra, gave the highest MOR and internal bonding. MOR depends on the bond strength in the polymer matrix, surface topology and lignocellulose material [70].

Discussion above clearly shows the interaction between cassava peels starch and lignocellulose material is measured by the size of the voids in particleboards. Voids are attributed to the interaction of carboxylic (-COOH) group in starch with hydroxyl (-OH) groups in lignin, cellulose and hemicellulose. Voids in particleboards explain the levels of reaction in lignocellulose materials and cassava peels starch. Smallest void were observed in the particleboards formulated from RH. This is due to the reaction of –COOH and –OH from cassava peel starch with hydroxyl groups from silicic acid, lignin, cellulose and hemicellulose. MS consists of hydroxyl groups from cellulose, hemicellulose and lignin that reacted with carboxylic and hydroxyl groups in starch molecules. SB had a higher content of lignin which implies that few hydroxyl groups used for reaction with carboxylic and hydroxyl groups in cassava starch. Hydrolized rice husk has more reaction sites compared with MS and SB.

5. Conclusion

Lignocellulose materials are copolymerized with cassava peel starch through covalent bondage formed through condensation reaction. Oxidation of starch converts C–OH to –COOH. The carboxylic group reacts with hydroxyl groups from lignin, cellulose and hemicellulose natural polymers through esterification and etherification in condensation polymerization that brings about molecular bonding during particleboard formulation. High lignin content results to low WA and TS. Its structure provides a higher MOE and MOR. Formulated particleboards from RH showed smallest sizes of voids are associated with interaction between carboxylic and hydroxyl from starch with hydroxyl from silicic acid, lignin, cellulose and hemicellulose, whereas for sugarcane bagasse showed largest void sizes had a higher content of lignin which implies that few hydroxyl groups used for reaction with carboxylic and hydroxyl groups in cassava starch. Silica (SiO_2) and NaOH reacts to form Na_2SiO_3 that hydrolysis to silicic acid. Silicic acid reacts with cassava peels through the silication process where hydroxyl groups from silicic acid with carboxylic groups from cassava peels starch. Crosslinking of starch with hydrolyzed borax through condensation reaction between hydroxyl groups from borate and lignocellulose material provides another major bond formation in particleboard formulation.

Declarations

Author contribution statement

Stephen W. Kariuki, Jackson W. Muthengia, Millien K. Erastus, Genson M. Leonard, Joseph M. Marangu: Conceived and designed the experiments; Performed the experiments; Analyzed and interpreted the data; Contributed reagents, materials, analysis tools or data; Wrote the paper.

Funding statement

This research did not receive any specific grant from funding agencies in the public, commercial, or not-for-profit sectors.

Competing interest statement

The authors declare no conflict of interest.

Additional information

Additional information for this paper will be availed on request.

References

[1] S.L. Oliveira, R.F. Mendes, L.M. Mendes, T.P. Freire, Particleboard panels made from sugarcane bagasse: characterization for use in the furniture industry, J. Mater. Res. 19 (2016) 914–922.

[2] J.K. Saini, R. Saini, L. Tewari, Lignocellulosic agriculture wastes as biomass feedstocks for second-generation bioethanol production: concepts and recent developments, J. Biotechnol. 5 (2014) 337–353.

[3] N.S. Cetin, N. Ozmen, Studies on lignin-based adhesives for particleboard panels, Journal for Turkish Agriculture and Forest 27 (2003) 183–189. http://dergipark.ulakbim.gov.tr/tbtkagriculture/article/view/5000028236.

[4] M. Ferreira, C. Miranda, M. Magalhães, A. Bispo, J. Oliveira, J. Silva, N. José, Starch-based films plasticized with glycerol and lignin from piassava fiber reinforced with nanocrystals from Eucalyptus, Mater. Today: Proceedings 2 (2015).

[5] D.H.S. Souza, C.T. Andrade, M.L. Dias, Effect of synthetic mica on the thermal properties of poly(lactic acid), Journal for Polímeros Ciência e Tecnologia 24 (2014) 20–24.

[6] K.F. Patel, H.U. Mehta, H.C. Srivastava, Kinetics and mechanism of oxidation of starch with sodium hypochloride, J. Appl. Polym. Sci. 399 (1974) 389–399.

[7] F. Xie, L. Yu, H. Liu, L. Chen, Starch modification using reactive extrusion, J. Starch 58 (2016) 131–139.

[8] C. Siau, A. Karim, M. Norziah, W. Wan Rosli, Effects of cationization on DSC thermal profiles, pasting and emulsifying properties of sago starch, J. Sci. Food Agric. 84 (2004) 1722–1730.

[9] Z. Qiao, J. Gu, S. Lv, J. Cao, H. Tan, Y. Zhang, Preparation and properties of normal temperature cured starch-based wood adhesive, J. BioResources 11 (2016) 4839–4849.

[10] M. Haroon, L. Wang, H. Yu, N.M. Abbasi, Z.A. Zain-ul-Abdin, M. Saleem, J. Wu, Chemical modification of starch and its application as an adsorbent material, J. RSC Advances 6 (2016) 78264–78285.

[11] V.G. Gayathri, S. Debnath, M.N. Babu, Chemically modified starches and their applications in pharmacy, J. Pharm Nano Science 2 (2013) 332–344.

[12] F.J. Polnaya, M.D.W. Haryadi, M.N. Cahyanto, Effects of phosphorylation and crosslinking on the pasting properties and molecular structure of sago starch, J. Food Res. 20 (2013) 1609–1615.

[13] M.V. Lawal, M.A. Odeniyi, O.A. Itiola, Material and rheological properties of native, acetylated and pregelatinized forms of corn, cassava and sweet potato starches, J. Starch/Stärke 67 (2015) 964–975.

[14] S.E. Barrios, J.M. Contreras, F. López-Carrasquero, A.J. Müller, Chemical modification of cassava starch by carboxymethylation reactions using sodium monochloro acetate as modifying agent, J. Revista de la Facultad de Ingenieria 27 (2012) 97–105.

[15] A. Gunaratne, Effect of heat–moisture treatment on the structure and physicochemical properties of tuber and root starches, J. Carbohydrate Polymers 49 (2002) 425–437.

[16] S.F. Chin, A. Azman, S.C. Pang, Size controlled synthesis of starch nanoparticles by a microemulsion method, J. Nanomater. 2014 (2014) 1–7.

[17] P. Wang, J.J. Kosinski, M.M. Lencka, A. Anderko, R.D. Springer, Thermodynamic modeling of boric acid and selected metal borate systems, J. Pure and Applied Chemistry 85 (2013) 2117–2144.

[18] L.V. Angelova, M. Leskes, B.H. Berrie, R.G. Weiss, Selective formation of organo, organo-aqueous, and hydro gel-like materials from partially hydrolysed poly(vinyl Acetate)s based on different boron-containing crosslinkers, J. Soft Matter 11 (2015) 5060–5066.

[19] S. Lepifre, S. Baumberger, B. Pollet, F. Cazaux, X. Coqueret, C. Lapierre, Reactivity of sulphur-free alkali lignins within starch films, J. Industrial Crops Products 20 (2004) 219–230.

[20] H.S.S. Shekar, M. Ramachandra, Green composites: a review, J. Materials Today: Proceed 5 (2018) 2518–2526.

[21] S. Baumberger, C. Lapierre, B. Monties, G.D. Valle, Use of kraft lignin as filler for starch films, J. Polymer Degradation Stability 59 (2010) 273–277.

[22] M.M. Rahman, A.N. Netravali, Advanced green composites using liquid crystalline cellulose fibers and waxy maize starch based resin, J. Composites Sci. Technol 162 (2018) 110–116.

[23] S. Narkchamnan, C. Sakdaronnarong, Thermo-molded biocomposite from cassava starch, natural fibers and lignin associated by laccase-mediator system, J. Carbohydrate Polym 96 (2013) 109–117.

[24] F. Jendoubi, A. Mgaidi, M. El Maaoui, Kinetics of the dissolution of silica in aqueous sodium hydroxide solutions at high pressure and temperature, J. Chem. Eng. 75 (1997) 721–727.

[25] P. Overton, E. Danilovtseva, E. Karjalainen, M. Karesoja, V. Annenkov, H. Tenhu, V. Aseyev, Water-dispersible silica-polyelectrolyte nanocomposites prepared via acid-triggered polycondensation of silicic acid and directed by polycations, J. Polymers 8 (2016) 96.

[26] J.H.M. Visser, Fundamentals of alkali-silica gel formation and swelling: condensation under influence of dissolved salts, J. Cement. Concrete Res 105 (2018) 18–30.

[27] L. Zhang, Y. Ding, J. Song, Crosslinked carboxymethyl cellulose-sodium borate hybrid binder for advanced silicon anodes in lithium-ion batteries, Chin. Chem. Lett. (2016).

[28] S.K. Warui, J. Wachira, M. Kawira, G.M. Leonard, Characterization of prototype formulated particleboards from agroindustrial lignocellulose biomass bonded with chemically modified cassava peel starch, J. Adv. Materi Sci. Engineering 2019 (2019) 1–15.

[29] P. Mischnick, D. Momcilovic, Chemical structure analysis of starch and cellulose derivatives, J. Advan Carbohydrate Chemistry Biochemistry 64 (2010) 117–210.

[30] K. Fagerstedt, P. Saranpaa, T. Tapanila, J. Immanen, J. Serra, K. Nieminen, Determining the composition of lignins in different tissues of silver birch, J. Plants 4 (2015) 183–195.

[31] J.B. Sluiter, R.O. Ruiz, C.J. Scarlata, A.D. Sluiter, D.W. Templeton, Compositional analysis of lignocellulosic feedstocks. 1. Review and description of methods, J. Agric. Food Chem. 58 (2010) 9043–9053.

[32] I.J. Opara, C.D. Ossi, C.O. OkoUdu, Formulation of cassava starch-based adhesive, Int. J. Adv. Res. 5 (2017) 26–33.

[33] A. Sluiter, J. Sluiter, E. Wolfrum, M. Reed, R. Ness, C. Scarlata, J. Henry, Improved methods for the determination of drying conditions and fraction insoluble solids (FIS) in biomass pretreatment slurry, Journal for Biomass and Bioenergy 91 (2016) 234–242.

[34] J. Yang, Y.C. Ching, C.H. Chuah, Applications of lignocellulosic fibers and lignin in bioplastics: a review, Journal for Polymers 11 (2019) 751.

[35] W. Zhou, D.N. Mahato, C.A. MacDonald, Analysis of powder X-ray diffraction resolution using collimating and focusing polycapillary optics, J. Thin Solid Films 518 (2010) 5047–5056.

[36] H. Ouhaddouch, A. Cheikh, M.O.B. Idrissi, M. Draoui, M. Bouatia, FT-IR spectroscopy applied for identification of a mineral drug substance in drug products: application to bentonite, J. Spectroscopy 2019 (2019) 1–6.

[37] A.A. Zarifa, M.A. Shammala, A.A. Sheikh, Sustainable manufacturing of particleboards from sawdust and agricultural waste mixed with recycled plastics, J. Environ. Eng. 8 (2018) 174–180.

[38] S.H. Imam, S.H. Gordon, L. Mao, L. Chen, Environmentally friendly wood adhesive from a renewable plant polymer: characteristics and optimization, J Polymer Degradation Stability 73 (2001) 529–533.

[39] S. Kalami, M. Arefmanesh, E. Master, M. Nejad, Replacing 100% of phenol in phenolic adhesive formulations with lignin, J. Appl. Polym. Sci. 134 (2017) 45124.

[40] G. Nemli, S. Demirel, E. Gumuskaya, M. Aslan, C. Acar, Feasibility of incorporating waste grass clippings (*Lolium perenne L.*) in particleboard composites, J. Waste Management 29 (2009) 1129–1131.

[41] H. Staroszczyk, P. Janas, Microwave-assisted preparation of potato starch silicated with silicic acid, J. Carbohydrate Polymers 81 (2010) 599–606.

[42] H. Chen, Chemical composition and structure of natural lignocellulose, J. Biotechnology of Lignocellulose (2014) 25–71.

[43] G. Lv, S. Wu, Analytical pyrolysis studies of corn stalk and its three main components by TG-MS and py-GC/MS, J. Anal. Appl. Pyrol. 97 (2012) 11–18.

[44] L. Hajji, A. Boukir, J. Assouik, A. Kerbal, M. Kajjout, P. Doumenq, M.L. De Carvalho, A multi-analytical approach for the evaluation of the efficiency of the conservation–restoration treatment of Moroccan historical manuscripts dating to the 16th, 17th, and 18th centuries, J. Appl. Spectrosc. 69 (2015) 920–938.

[45] A. Mandal, D. Chakrabarty, Isolation of nanocellulose from waste sugarcane bagasse (SCB) and its characterization, J. Carbohydrate Polymers 86 (2011) 1291–1299.

[46] U. Uthumporn, Y.N. Shariffa, A. Fazilah, A.A. Karim, Effects of NaOH treatment of cereal starch granules on the extent of granular starch hydrolysis, J. Colloid and Polymer Science 290 (2012) 1481–1491.

[47] R.A. Bakar, R. Yahya, S.N. Gan, Production of high purity amorphous silica from rice husk, J. Procedia Chem 19 (2016) 189–195.

[48] I.J. Fernandes, D. Calheiro, F.A.L. Sanchez, A.L.D. Camacho, T.L.A.d.C. Rocha, C.A.M. Moraes, V.C.d. Sousa, Characterization of silica produced from rice husk ash: comparison of purification and processing methods, J. Mater. Res. 20 (2017) 512–518.

[49] C.M. Paranhos, J.A. Santana Costa, Systematic evaluation of amorphous silica production from rice husk ashes, J. Clean. Prod. 192 (2018) 688–697.

[50] X. Zhou, W. Li, L. Zhu, H. Ye, H. Liu, Polymer–silica hybrid self-healing nano/microcapsules with enhanced thermal and mechanical stability, J. RSC Advances 9 (2019) 1782–1791.

[51] H. Lei, A. Pizzi, P. Navarrete, S. Rigolet, A. Redl, A. Wagner, Gluten protein adhesives for wood panels, J. Adhes. Sci. Technol. 24 (2010) 1583–1596.

[52] T.Q. Yuan, S.N. Sun, F. Xu, R.C. Sun, Structural characterization of lignin from triploid of populus tomentosa carr, J. Agric. Food Chem. 59 (2011) 6605–6615.

[53] R. El Hage, N. Brosse, L. Chrusciel, C. Sanchez, P. Sannigrahi, A. Ragauskas, Characterization of milled wood lignin and ethanol organosolv lignin from miscanthus, Polym. Degrad. Stabil. 94 (2009) 1632–1638.

[54] A.E. Capanema, Y.M. Balakshin, F.J. Kadla, Quantitative characterization of a hardwood milled WoodLignin by nuclear magnetic resonance spectroscopy, J. Agric. Food Chem. 53 (2005) 9639–9649.

[55] E.L. Hult, P.T. Larsson, T. Iversen, A comparative CP/MAS 13C-NMR study of the supermolecular structure of polysaccharides in sulphite and kraft pulps, Journal for Holzforschung 56 (2002) 179–184.

[56] H.M. Hazwan, A.A. Aziz, A. Iqbal, M.N.M. Ibrahim, N.H.A. Latif, Development and characterization novel bio-adhesive for wood using kenaf core (Hibiscus cannabinus) lignin and glyoxal, J. Biological Macromolecules 122 (2019) 713–722.

[57] I. Tan, B.M. Flanagan, P.J. Halley, A.K. Whittaker, M.J. Gidley, A method for estimating the nature and relative proportions of amorphous, single, and double-helical components in starch granules by13C CP/MAS NMR, J. Biomacromolecules 8 (2007) 885–891.

[58] Y. Qin, H. Zhang, Y. Dai, H. Hou, H. Dong, Effect of alkali treatment on structure and properties of high amylose corn starch film, J. Mater. 12 (2019) 1705.

[59] R. Spaccini, D. Todisco, M. Drosos, A. Nebbioso, A. Piccolo, Decomposition of biodegradable plastic polymer in a real on-farm composting process, J.Chem. Biological Technol Agri 3 (2016) 1–12.

[60] J.X. Sun, X.F. Sun, H. Zhao, R.C. Sun, Isolation and characterization of cellulose from sugarcane bagasse, J. Polymer Degradation Stability 84 (2004) 331–339.

[61] C. Rezende, M. de Lima, P. Maziero, E. deAzevedo, W. Garcia, I. Polikarpov, Chemical and morphological characterization of sugarcane bagasse submitted to a

delignification process for enhanced enzymatic digestibility, J. Biotechnology for Biofuels 4 (2011) 54.
[62] M. Sujka, J. Jamroz, Characteristics of pores in native and hydrolyzed starch granules, J. Starch - Stärke 62 (2010) 229–235.
[63] M. Tako, S. Hizukuri, Gelatinization mechanism of potato starch, J. Carbohydrate Polymers 48 (2002) 397–401.
[64] H. Yamamoto, E. Makita, Y. Oki, M. Otani, Flow characteristics and gelatinization kinetics of rice starch under strong alkali conditions, J. Food Hydrocolloids 20 (2006) 9–20.
[65] M.B. Cardoso, From Rice Starch to Amylose Crystals: Alkaline Extraction of Rice Starch, Solution Properties of Amylose and Crystal Structure of V-Amylose Inclusion Complexes, Université Joseph Fourier, Grenoble I, France, 2007.
[66] T.C. Mokhena, M.J. Mochane, T.E. Motaung, L.Z. Linganiso, O.M. Thekisoe, S.P. Songca, Sugarcane bagasse and cellulose polymer composites, Sugarcane Technology. Research (2018).
[67] T. Williams, M. Hosur, M. Theodore, A. Netravali, V. Rangari, S. Jeelani, Time effects on morphology and bonding ability in mercerized natural fibers for composite reinforcement, J. Polym. Sci. 2011 (2011) 1–9.
[68] A. Potthast, T. Rosenau, P. Kosma, Analysis of oxidized functionalities in cellulose, J. Polym. Sci. 205 (2006) 1–48.
[69] E.M. Ciannamea, P.M. Stefani, R.A. Ruseckaite, Medium-density particleboards from modified rice husks and soybean protein concentrate-based adhesives, J. Bioresource Technology 101 (2010) 818–825.
[70] A.S. Singha, V.K. Thakur, Mechanical, morphological, and thermal characterization of compression-molded polymer biocomposites, J. Polymer Analysis Characterization 15 (2010) 87–97.